Direct Detection of Nonlinear Ferromagnetic Resonance in Thin Films by the Magneto-Optical Kerr Effect

Thomas Gerrits,[1] Pavol Krivosik,[2,3] Michael L. Schneider,[1] Carl E. Patton,[2] and T. J. Silva[1]

[1]*National Institute of Standards and Technology, Boulder, Colorado 80305, USA*
[2]*Department of Physics, Colorado State University, Fort Collins, Colorado 80523, USA*
[3]*Slovak University of Technology, 812 19 Bratislava, Slovak Republic*

The longitudinal magneto-optical Kerr effect is used to obtain a calibrated measure of the dynamic magnetization response over the ferromagnetic resonance (FMR) profile for in-plane magnetized Permalloy films excited with high power in-plane transverse microwave fields at 1.25 to 3.75 GHz and in-plane precession angles up to about 20°. The data provide a profound demonstration of the Suhl threshold effect for parametric spin wave generation for angles above about 14°, the magnetization precession lock-up just above threshold, and the complicated response over the full FMR profile at very high powers.

Ferromagnetic resonance (FMR) can be separated into two regimes. First, there is the low power small angle response regime that can be described by a linearized damped precession model [1]. Second, there is the high power and generally larger angle response regime that involves Suhl spin wave instability processes and threshold effects [2]. The thresholds can occur at precession angles at fractions of a degree for some single-crystal ferrites [3], or tens of degrees for metallic thin films [4,5].

With the exception of inductive pick-up loop techniques used for some of the early high power work on microwave ferrites [6], the nonlinear Suhl response has generally been inferred from microwave cavity measurements [4]. In recent years, however, new coplanar waveguide (CPW) techniques have been developed to study the FMR response, particularly for metallic ferromagnetic films, in the time domain with step field excitation [7,8] and in the field or frequency domain with cw microwave excitation [1,9]. While CPW excitation is highly attractive for nonlinear dynamics studies, the time domain FMR response to fast rise time step fields does not appear to produce parametric spin waves or show Suhl instability effects, even when the dynamic magnetization deflection angles are in excess of 90° [10,11]. Recent time-resolved FMR measurements on Permalloy films made with large amplitude microwave pulses, however, do indicate a substantial increase in the apparent damping as well as a decrease in the spatially averaged magnetization [12]. These are precisely the effects associated with Suhl processes. Recent work has also demonstrated the use of magneto-optical methods for FMR measurements [13–15].

This Letter reports on a technique for the direct measurement of the quantitative magnetization dynamics associated with nonlinear ferromagnetic resonance (NLFMR) in a thin film under cw microwave excitation in a CPW structure. The method involves a new quantitative analysis of the nonlinear response, obtained by direct longitudinal

magneto-optic Kerr effect (MOKE) measurements of the change in the longitudinal component of the magnetization M_z as a function of the static field, frequency, and microwave field amplitude.

By way of example, specific results are given below for a 20 nm thick Permalloy film and a range of microwave excitation frequencies from 1.25 to 3.75 GHz. The data show the classic near uniform mode linear FMR response for powers below the Suhl threshold, a lock-up in the precession cone at and just above the threshold, and the complicated nonlinear response that occurs at high power. The MOKE-NLFMR method gives quantitative information on the critical precession angle and microwave field amplitude at the onset of the Suhl instability. In combination with theory, the data also yield a determination of the spin wave relaxation rate for the critical modes. One special advantage of the MOKE-NLFMR technique is that the Suhl processes, both at and above threshold, can be identified directly.

The threshold microwave field amplitude for this process, h_{crit}, may be written as

$$h_{\mathrm{crit}} = \Delta H_{\mathrm{FMR}} \left(\frac{2\eta_k}{W_k \omega_M} \right)^{1/2}. \tag{1}$$

Here, ΔH_{FMR} is the half-power FMR field swept linewidth and η_k denotes the relaxation rate of the critical spin wave mode. The real positive dimensionless W_k parameter reflects the coupling between the uniform mode and the critical spin wave mode for the thin film geometry [16]. W_k is generally a function of the film parameters, the field, and the frequency. In the present case, W_k is in the 0.1–0.4 range, depending on the pumping frequency. The parameter $\omega_M = \mu_0 |\gamma| M_s$ expresses the saturation magnetization of the film, M_s, in frequency units. Here, μ_0 and γ denote the permeability of free space and the electron gyromagnetic ratio, respectively. Equation (1) shows that a mea-

surement of h_{crit}, coupled with a proper theoretical evaluation of W_k, can yield a determination of the critical mode spin wave relaxation rate. This is one of the key realizations from the Suhl theory.

The 20 nm thick $Ni_{80}Fe_{20}$ films were sputter deposited on glass in an in-plane field of 20 kA/m (250 Oe) to define the uniaxial anisotropy easy axis. This ensures a symmetric response around the equilibrium axis even at low bias fields and large pump fields when the bias field is aligned parallel to the easy axis. The films were capped with a 12 nm silicon nitride protective overcoat. Standard magnetometry gave a saturation induction $\mu_0 M_s$ value of 1.07 T (10.7 kG).

The experimental arrangement is shown in Fig. 1. The sample was placed film side down on a CPW structure with the film easy axis parallel to the static field **H** and the CPW line axis, as indicated. The film was insulated from the CPW structure with a 1 mm polyimide layer. The microwave pump field **h** was applied through the application of 1 kHz square-wave modulated microwave power to the signal line. The amplitude (h) of the pump field was calibrated from the voltage at the CPW output. We measured the magnetization response across the center conductor and found a homogeneous response until close to the edges, where the pump field direction changes from in-plane to out-of-plane.

The longitudinal MOKE setup was composed of an s polarized 800 nm, 4 mW laser beam focused to a 20 μm diameter spot size at the sample, a standard polarization analyzer, a photodiode, and a lock-in amplifier for detection. The magnetization M_z component serves to rotate the plane of polarization of the incident beam slightly, but with little if any elliptical distortion. The M_y component makes no contributions to the polarization change to first order, as we probe the magnetization with incoming s polarization.
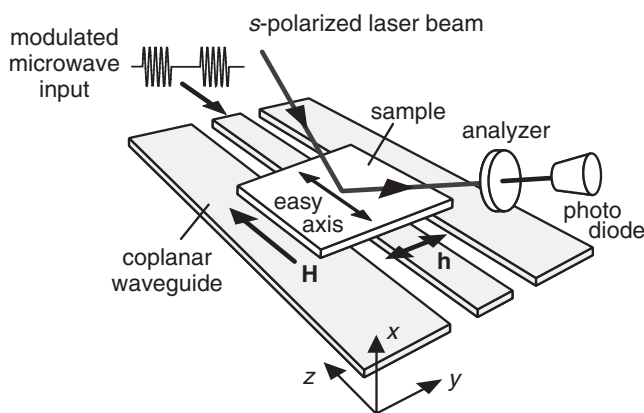

FIG. 1. Schematic of experiment. The thin film is placed on top of a coplanar waveguide (CPW) structure with the film easy axis and the static applied field **H** parallel to the CPW line and the z direction. The field **h** is generated by the CPW line and the modulated microwave input. The longitudinal magneto-optical Kerr effect detection scheme is shown schematically by the s-polarized laser beam, the analyzer, and the photodiode.

The polar MOKE M_x signal, as well as the quadratic contribution of $M_x \cdot M_y$, average to zero because of the low 10 kHz bandwidth of the photodiode that is far below the nominal 1–4 GHz range of FMR excitation frequencies in the experiments. Possible polarization rotation contributions originating from the glass substrate are subtracted by the nature of the lock-in detection technique. For Permalloy films with an angle of incidence of 45°, the maximum Kerr rotation for a full magnetization reversal is about 500 μrad. For an analyzer setting at 1° off the crossed polarizer-analyzer configuration as used here, the output light intensity is approximately linear in M_z.

Because of the nanosecond time scale for the FMR response and the anticipated parametric Suhl response, in combination with the low bandwidth of the photodiode, the detected signal will correspond to the change in the time averaged z component of the magnetization, taken as $\Delta\langle M_z \rangle$, between the power on and power off time intervals of the square-wave modulation. The raw signals were calibrated against the maximum possible MOKE response obtained by alternatively saturating the film in the $\pm z$ directions. This was done by the application of a symmetric 4.8 kA/m (60 Oe) peak-to-peak square-wave field drive at 2 Hz. The calibrated signal then corresponds to $\Delta\langle M_z \rangle / M_s$. For in-plane magnetized Permalloy films and the range of microwave frequencies used here, the precession cone is effectively flat and constrained to lie in the y-z plane, as defined in Fig. 1. The maximum change in the magnetization z component ΔM_z over a precession cycle, taken as ΔM_z, is then close to $2\Delta\langle M_z \rangle$ and the in-plane precession angle is equal to $\cos^{-1}(1 - \Delta M_z / M_s)$.

Full sets of $\Delta M_z / M_s$ vs H profiles that correspond to the FMR response were obtained for h values from about 70 to 400 A/m (0.9 to 5.0 Oe). The FMR field H_R was obtained as the maximum response point on a given $\Delta M_z / M_s$ vs H profile at low power. The $H_R(\omega)$ response generally matched the thin film FMR condition in the low frequency limit, $\omega = |\gamma|\mu_0[(H_R + H_k)M_s]^{1/2}$, where H_k is the uniaxial anisotropy field. Fits to this relation gave $|\gamma|$ and H_k values consistent with field-deposited Permalloy films.

Figure 2 gives results for the frequency $\omega/2\pi = 2.25$ GHz. Similar results were found at other frequencies. Figure 2(a) shows $\Delta M_z / M_s$ vs H profiles for the full range of h values noted above. The solid circles identify the maximum $\Delta M_z / M_s$ points from curve to curve. Under the assumption of a constant overall magnetization vector, generally valid only at low power, the numbers on the vertical axis give in-plane precession angles from about 8° at $\Delta M_z / M_s = 0.01$ to about 20° at $\Delta M_z / M_s = 0.06$. The break in the data at $\Delta M_z / M_s \approx 0.03$ and $h = h_{crit} \approx 130$ A/m (1.6 Oe) corresponds to the Suhl threshold. The in-plane precession angle at this point is about 14°. The corresponding critical ΔM_z value, taken as ΔM_{zc}, is close to $0.03 M_s$. For h values below 120 A/m (1.5 Oe), the $\Delta M_z(H)$ profiles translate into transverse magnetization amplitude $|m_y(H)|$ response that closely matches linear FMR theory.
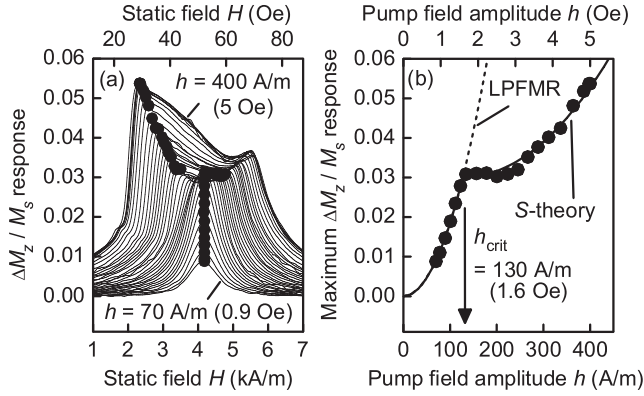
FIG. 2. (a) Collage of profiles of the measured change in the longitudinal magnetization component ΔM_z, normalized to the magnetization M_s, as a function of the static field H for a range of microwave field amplitude h values, as indicated. The maximum values at a given h are shown by the solid circles. (b) Maximum $\Delta M_z/M_s$ values from (a) versus h, with fitted curves from low power FMR (LPFMR) theory and the nonlinear S theory, as indicated. The microwave frequency was 2.25 GHz.

Figure 2(b) shows the maximum $\Delta M_z/M_s$ points from Fig. 2(a) as a function of h. The solid circles show the data. There are three distinct regions: (i) There is a smooth quadratic increase for h values below h_{crit}; (ii) there is an apparent lock-up in ΔM_z at ΔM_{zc} as h moves from h_{crit} up to about 200 A/m (2.5 Oe); (iii) as h moves to higher h values, the increase in $\Delta M_z/M_s$ resumes. The quadratic increase at low h is related to the linear FMR response. Both the lock-up and resumed increase for $h \gtrsim h_{crit}$ relate to the Suhl NLFMR response. As these data show, the MOKE-NLFMR technique makes all of these responses accessible by simple and direct experimental means, and in a form that is amenable to ready analysis.

Consider the low power response in somewhat more detail. When the anisotropy easy axis is aligned parallel to the bias field direction the transverse m_y response will be linear in h. In the small signal limit, with $|\mathbf{M}| = M_s$ and $|m_y| \ll M_s$, one can write $\Delta M_z/M_s \approx |m_y|^2/2M_s^2$. The theoretical low power FMR (LPFMR) $\Delta M_z(h)$ response, therefore, is quadratic in h. The dashed LPFMR labeled line in Fig. 2(b) shows a quadratic fit to the data for $h < 130$ A/m. The linear theory gives an overall LPFMR response with $|m_y| \approx 2M_s h/\Delta H_{FMR}$ and $\Delta M_z/M_s \approx 2h^2/\Delta H_{FMR}^2$. The fit shown corresponds to an FMR linewidth of 980 A/m (12.2 Oe). This value matches the half-power linewidth obtained directly from the low power $|m_y(H)|$ profiles for $h < h_{crit}$.

The lock-up and the high power $\Delta M_z/M_s$ vs h response are related to the above-threshold steady-state dynamics. Various approaches have been used to model this type of nonlinear response. These include a back reaction of the parametric spin waves on the FMR mode [2], nonlinear damping associated with the spin waves [17], and a phase limiting mechanism through what is often called the S theory [18].

Following L'vov [19], the S theory yields a working equation for ΔM_z above threshold of the form:

$$R\frac{\Delta M_z}{\Delta M_{zc}} + \sqrt{\left(\frac{\Delta M_z}{\Delta M_{zc}}\right)^2 - 1} = R\frac{h}{h_{crit}}\sqrt{\frac{\Delta M_z}{\Delta M_{zc}}}. \quad (2)$$

The R parameter controls the level of the phase limitation and is on the order of unity. In physical terms, this limitation is due to a power dependent change in phase between the pair of parametrically excited spin waves and the microwave field that results in a decrease in the effective pumping power. There is no phase limitation for $R = 0$ and the lock-up would remain constant at $\Delta M_z = \Delta M_{zc}$. For a very large R, parametric spin wave excitation would be suppressed at any power. The S theory curve in Fig. 2 was obtained for $\Delta M_{zc}/M_s = 0.03$, $h_{crit} = 130$ A/m, and $R = 0.6$. One can see that Eq. (2) models the above-threshold data extremely well with a moderate choice of R. Applications of the first two approaches cited above do not give acceptable fits to the data. Taken more generally, these results may well be an indication that the phase limitation mechanism also plays a dominant role in the large angle dynamic magnetization response in metallic thin films.

Figure 3 summarizes key results for all frequencies. Figures 3(a) and 3(b) show the ΔH_{FMR} and h_{crit} versus frequency results. The lines show linear fits. Figure 3(c) shows the theoretical variation in W_k with frequency from the S theory. The solid circles in Fig. 3(d) show final results on the spin wave relaxation rate η_k versus frequency, based on Eq. (1) and the results in Figs. 3(a)–3(c). As a basis of comparison, the open circles in 3(d) show the uniform mode relaxation rate η_0 versus frequency, and the horizontal line shows the mean η_0 value. The linear frequency dependence for ΔH_{FMR} in Fig. 3(a) is typical for metallic thin films [1]. The slope of the linear fit corresponds to a Gilbert damping parameter α value of about 0.005. The zero-frequency linewidth intercept at $\Delta H_{inh} = 302$ A/m (3.8 Oe) can be ascribed to inhomogeneous line broadening. One can see that the h_{crit} response in 3(b) is also more or less linear in frequency. When combined with the nearly linear W_k versus frequency response in 3(c), along with the effects of the nonzero intercepts in 3(a)–3(c), the end result is an η_k that appears to be relatively level for $\omega/2\pi > 2.5$ GHz, and drops off at lower frequencies.

The correlation between the η_k results and the intrinsic FMR relaxation rate η_0 is significant. The open circle points come from the working equation that connects the assumed intrinsic FMR linewidth, $\Delta H = \Delta H_{FMR} - \Delta H_{inh}$, to α in the narrow linewidth limit, namely $\Delta H = 2\alpha\omega/|\gamma|$, in combination with the relaxation rate connection applicable in the low frequency limit, $\eta_0 \approx \alpha\omega_M/2$ [1].

The results in Fig. 3(d) indicate that the critical spin wave mode relaxation rate is more or less frequency independent and very close to the intrinsic uniform mode relaxation rate for frequencies above 2.5 GHz. This indi-
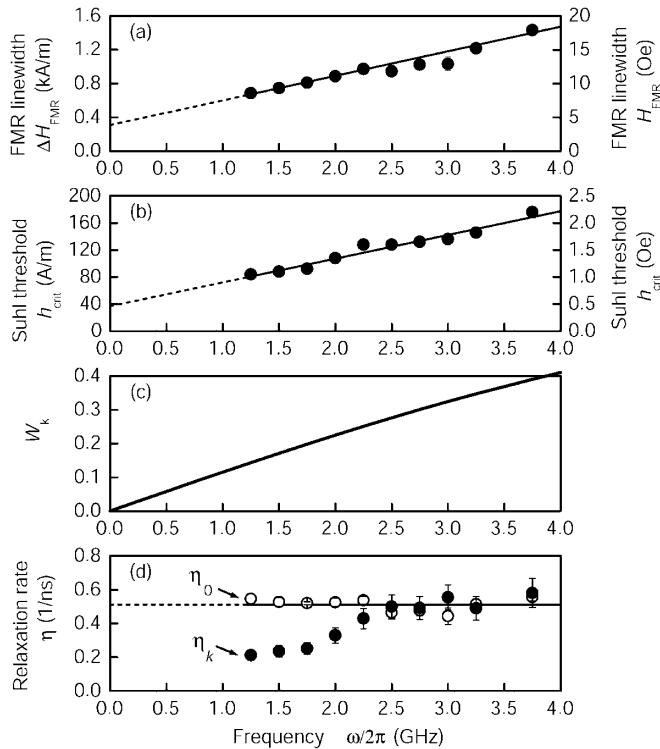
FIG. 3.   (a)–(d) show, respectively, the low power FMR linewidth ΔH_{FMR}, the threshold field h_{crit}, the theoretical critical mode coupling factor W_k, and the extracted spin wave relaxation rate η_k versus frequency. The lines in (a) and (b) show a linear fit. (d) also shows the uniform mode relaxation rate η_0 versus frequency.

cates that both the spin wave relaxation rate from the Suhl threshold data and the α-based uniform mode relaxation rate have a common origin. Suhl instability is generally taken to depend on intrinsic relaxation rates. The clear match up between η_k and η_0, therefore, supports a conclusion that both are due to the magnon-electron relaxation processes that are generally accepted as the source of the intrinsic ferromagnetic relaxation in metals [20]. For frequencies below 2.5 GHz, interestingly, η_k appears to drop off. The important point for this Letter, as noted earlier, is that MOKE-NLFMR allows one to access these behaviors in a direct way. Significant work remains to fully understand the ramifications of these spin wave loss parameters and connections with the FMR loss.

In summary, a new MOKE based analysis for direct nonlinear FMR measurements has been developed. The data reveal a wide range of spin wave instability effects that include clear signatures for the second order Suhl threshold h_{crit} and the above-threshold steady-state response. The h_{crit} values are consistent with fundamental relaxation rate considerations. The response above threshold can be well modeled in terms of dephasing effects, as quantified through the S theory of Zakharov and L'vov.

[1] See, for example, S. S. Kalarickal, M. Wu, P. Krivosik, C. E. Patton, M. L. Schneider, P. Kabos, T. J. Silva, and J. P. Nibarger, J. Appl. Phys. **99**, 093909 (2006).
[2] H. Suhl, J. Phys. Chem. Solids **1**, 209 (1957).
[3] M. Chen and C. E. Patton, *Nonlinear Phenomena and Chaos in Magnetic Materials*, edited by P. E. Wigen (World Scientific, Singapore, 1994).
[4] See, for example, S. Y. An, P. Krivosik, M. A. Kraemer, H. M. Olson, A. V. Nazarov, and C. E. Patton, J. Appl. Phys. **96**, 1572 (2004).
[5] H. M. Olson, P. Krivosik, K. Srinivasan, and C. E. Patton, in Technical Digest of the IEEE International Magnetics Conference, San Diego, CA, 2006 (IEEE, New York, to be published), p. 77.
[6] N. Bloembergen and S. Wang, Phys. Rev. **93**, 72 (1954).
[7] T. J. Silva, C. S. Lee, T. M. Crawford, and C. T. Rogers, J. Appl. Phys. **85**, 7849 (1999).
[8] R. Lopusnik, J. P. Nibarger, T. J. Silva, and Z. Celinski, Appl. Phys. Lett. **83**, 96 (2003).
[9] G. Counil, J. V. Kim, T. Devolder, C. Chappert, K. Shigeto, and Y. Otani, J. Appl. Phys. **95**, 5646 (2004).
[10] Th. Gerrits, H. A. M. van den Berg, J. Hohlfeld, L. Bär, and Th. Rasing, Nature (London) **418**, 509 (2002).
[11] Th. Gerrits, T. J. Silva, J. P. Nibarger, and Th. Rasing, J. Appl. Phys. **96**, 6023 (2004).
[12] Th. Gerrits, M. L. Schneider, A. B. Kos, and T. J. Silva, Phys. Rev. B **73**, 094454 (2006).
[13] R. Meckenstock, M. Möller, and D. Spoddig, Appl. Phys. Lett. **86**, 112506 (2005).
[14] M. Möller, D. Spoddig, and R. Meckenstock, J. Appl. Phys. **99**, 08J310 (2006).
[15] K. Gnatzig, H. Dötsch, M. Ye, and A. Brockmeyer, J. Appl. Phys. **62**, 4839 (1987).
[16] P. Krivosik, K. Srinivasan, H. M. Olson, and C. E. Patton, in Technical Digest of the IEEE International Magnetics Conference, San Diego, CA, 2006 (IEEE, New York, to be published), p. 70.
[17] J. D. Bierlein and P. M. Richards, Phys. Rev. B **1**, 4342 (1970).
[18] V. E. Zakharov, V. S. L'vov, and S. S. Starobinets, Sov. Phys. Usp. **17**, 896 (1975).
[19] V. S. L'vov, *Wave Turbulence Under Parametric Excitation* (Springer-Verlag, Berlin, 1994).
[20] V. Kambersky and C. E. Patton, Phys. Rev. B **11**, 2668 (1975).